Advances in Applied Mathematics and Mechanics
Adv. Appl. Math. Mech., Vol. **3**, No. 3, pp. 327-353

DOI: 10.4208/aamm.10-10s2-05
June 2011

Thermal Radiation Modelling in Tunnel Fires

Paolo Ciambelli, Maria Grazia Meo, Paola Russo*and
Salvatore Vaccaro

Department of Industrial Engineering, University of Salerno, via Ponte don Melillo 84084 Fisciano (SA), Italy

Received 11 January 2010; Accepted (in revised version) 4 November 2010

Available online 28 February 2011

Abstract. Modelling based on Computational Fluid Dynamics (CFD) is by now effectively used in fire research and hazard analysis. Depending on the scenario, radiative heat transfer can play a very important role in enclosure combustion events such as tunnel fires. In this work, the importance of radiation and the effect of the use of different approaches to account for it were assessed. Firstly, small-scale tunnel fire simulations were performed and the results compared with experimental data, then realistic full-scale scenarios were simulated. The results show up the capability of CFD modelling to reproduce with good approximation tunnel fires. Radiation proved to be noteworthy mainly when the scale of the fire is relatively large. Among the various approaches employed to simulate radiation, the use of the Discrete Transfer model gave the most accurate results, mainly when the absorption-emission characteristics of the combustion products were taken into account. Finally, the suitability of the use of CFD in quantitative Fire Hazard Analysis is discussed.

AMS subject classifications: 68U20

Key words: CFD, radiation modelling, fire hazard analysis, tunnel fires.

1 Introduction

Quantitative fire hazard analysis is becoming the fundamental tool of modern fire safety engineering practice, and it can help to evaluate and reduce the fire risk in industrial, civil or transport (i.e., road and rail tunnels) enclosures. Fire accidents in road tunnels have recently proven to be extremely costly in terms of human lives, but also in increased congestion, pollution and repairs [1]. The serious threat for lives mainly derives from high temperatures, toxic species, obscuration by smoke and, rad-

*Corresponding author.
URL: `www.diin.unisa.it`
Email: pciambelli@unisa.it (P. Ciambelli), mgmeo@unisa.it (M. G. Meo), parusso@unisa.it (P. Russo), svaccaro@unisa.it (S. Vaccaro)

iative heat flux. On the other hand, tunnel closure consequent to fires is prejudicial to national and international economy because it increases transport costs, reduces competitiveness and negatively impacts road safety. The goal of a Fire Hazard Analysis (FHA) is to determine the expected outcome of a specific set of conditions called fire scenario, either in order to find out the hazards that are present in an existing or planned tunnel, or for design and evaluation of the effectiveness of trial fire protection strategies. A tunnel fire scenario includes any details that have an effect on the outcome of interest. This outcome determination can be made by expert judgment, by probabilistic methods using data from past incidents, or by deterministic means such as fire models. The last include empirical correlations, computer programs, full-scale and reduced-scale models, and other physical models [2]. Although empirical correlations and simplified computer models allow a rapid assessment of a fire scenario, because quickly yield a value of the variables of interest, they are heavily limited by experimental conditions and simplifying assumptions [2,3].

In this context, the use of Computational Fluid Dynamics (CFD) techniques may represent an effective way to account for case and site specific details. These codes use a discretisation method in order to approximate the differential flow equations by a system of algebraic equations and solve the simplified balance equations for the conservation of mass, momentum, energy and gas species within the physical domain of interest, thus allowing the estimation of the transient flow patterns of the fire-induced air velocity, temperature, pollutants and smoke concentration in large and complex enclosures. A detailed insight into CFD methodology can be widely found in the literature, e.g., by Shaw [4], Lea [5], Gobeau et al. [3]. In the case of tunnels, CFD modelling for FHA can efficiently be used to evaluate the effects of changes in structural design and ventilation, or to assess performance of safety measures over a range of fires differing in size, duration and locations [3].

Tunnel fires, as fires in enclosures, are very complex in nature [6]. Their complexity arises from the fact that the physical and chemical processes (e.g., turbulence, combustion, radiation, etc) controlling fire and smoke development interact with each other and with the surroundings. Radiation can be a significant portion of the overall heat transfer in confined combusting flows, typically when temperatures are above 670K [3].

In fire science literature thermal radiation has been early recognized as an important and sometime dominant mode of heat transfer for medium and large scale fires. Indeed, it can determine the growth and spread of some type of fires [7,8]. Many authors [3,9–11] reported that radiative heat transfer can account for 20-40% of the heat output of a large fire. Combustion products such as CO_2 and H_2O, emitting energy in discrete bands, are the main radiation sources. Moreover, according to the review performed by Novozhilov [7], radiation due to luminous diffusion flames contributes significantly in lowering the flame temperatures. Finely dispersed soot particles act accordingly as individual minute black or gray body and emit continuously over a wide range of wavelengths. Soot, CO_2 and H_2O are responsible for more than 95% of the radiant absorption and emission [7]. Radiative heat transfer occurs between the

emitters and receivers, i.e., between solid surfaces, soot/gas phase mixtures of flames and smoke aerosols [12,13].

Sacadura [8] reports a detailed review of the various approaches to thermal radiation modelling in the most common CFD fire codes, with different levels of accuracy ranging from roughly simplified analyses to sophisticated methods of investigation. Moreover, he highlighted that very limited information is reported on the method used for radiative heat transfer calculations in a number of papers on CFD fire modelling and that, for a widespread use of accurate radiation models in current fire CFD codes, the key factor is the optimization of their accuracy/computing time ratios. Keramida et al. [14] compared the discrete transfer and the six-flux model for fire simulation, and found that the simple six-flux model suffices for small compartment fires, up to 100kW, whereas for higher heat release rates the Discrete Transfer can provide sufficient accuracy. A comprehensive comparison of six CFD computational methods for solution of the radiative transfer equation is reported by Jensen et al. [15] for the numerical simulation of a 2m diameter JP-8 pool fire. The authors found that inside the fire, where radiation is isotropic, all methods gave comparable results with good accuracy; on the whole, predictions of Discrete Transfer method agreed well with those of the Monte Carlo method which are considered as reference solutions. An in-depth discussion on the CFD models for modeling radiation is also available in literature [3,16–18].

Generally speaking, for cases ranging from transparent to optically thick regions, like fire, the Discrete Transfer and the Monte Carlo models accurately represent the solution of the radiative transfer equation.

In this work the *CFX* code by *ANSYS* [19] was used to evaluate the effect of different approaches and models employed to simulate thermal radiation on the conditions established in a tunnel when a gasoline pool fire occurs. In particular, the fractional heat loss approximation, the Discrete Transfer and the Monte Carlo models were used for the simulations. The radiation transport mode was also assessed, i.e., assuming that radiative flux transfers heat only "surface to surface", or that the domain fluid emits/absorbs radiation too. In the "participating media" mode the absorption-emission characteristics of the combustion products were either modelled by a constant absorption coefficient (Grey model) or by a Multigrey model, to account for the dependence on the local gas composition.

Indeed, in the case of the assumption of the Grey model all radiation quantities are uniform throughout the spectrum; instead, in the case of the Multigrey model gas absorption is represented by a weighted sum of grey media as a function of temperature, the partial pressure and the path length.

Finally, in the perspective of CFD use for Fire Hazard Analysis, simulation results in terms of incident radiation were also compared with results from empirical correlations available in the literature to assess radiant heat flux from a fire to a target fuel ("solid flame radiation model" [20]). Moreover, in the context of FHA the full-scale tunnel fire was also studied from the point of view of duration in the time of safety conditions within the tunnel.

2 The mathematical models

2.1 CFD fundamentals and physical sub-models

In a fire the main physical mechanisms involved are turbulence, buoyancy, wall heat transfer, combustion and radiation. The relevant simplified sub-models are computed and solved in coupling with the main governing equations, that is: (i) the continuity equation; (ii) the momentum equation; (iii) the energy equation.

The continuity equation is based on the principle of conservation of mass:

$$\frac{\partial \rho}{\partial t} + \nabla \cdot (\rho \mathbf{u}) = 0, \tag{2.1}$$

where t is the time, ρ the density and $\mathbf{u}$ the velocity vector.

Newton's second law of motion states that the rate of change of momentum of the fluid in the volume is equal to the sum of forces acting on it:

$$\frac{\partial (\rho \mathbf{u})}{\partial t} + \nabla \cdot (\rho \mathbf{u} \times \mathbf{u}) = -\nabla p + \rho \mathbf{g} + \mathbf{S} + \nabla \cdot \boldsymbol{\tau}, \tag{2.2}$$

where p is the pressure, $\mathbf{g}$ is the gravitational vector, $\mathbf{S}$ are all other external forces and $\boldsymbol{\tau}$ is the stress tensor.

The energy equation is derived from the first law of thermodynamics:

$$\frac{\partial (\rho h)}{\partial t} + \nabla \cdot (\rho h \mathbf{u}) = \frac{Dp}{Dt} + \dot{Q}_R - \nabla \cdot \mathbf{q_r} + \nabla \cdot (k \nabla T) + \sum_j \nabla \cdot (h_j \rho D_j \nabla Y_j), \tag{2.3}$$

where $h = \sum_j h_j Y_j$ is the enthalpy of the fluid and Y_j and h_j are the mixture fraction and the enthalpy of the j-th species, respectively, Dp/Dt is the material derivative of p, $\dot{Q}_R$ is the heat release rate per unit volume from chemical reactions, $\mathbf{q_r}$ the radiative heat flux, k the thermal conductivity, T the temperature and D_j is the diffusion coefficient for the j-th species into air.

2.1.1 Turbulence modelling

Turbulent mixing is the key process responsible for transport of heat, mass and momentum in the vast majority of fluid flows. Turbulent flows contain a wide range of length and time scales. The Reynolds Averaged Navier-Stokes equations (RANS) are produced considering a generic property of a flow, such as the component u_i of velocity at a certain point, to consist of fluctuating part u_i' (due to turbulence) and a non-fluctuating part $\overline{u}_i$ [4]:

$$u_i = \overline{u}_i + u_i'. \tag{2.4}$$

Upon averaging the equations new unknown terms appear. These terms are referred to as the "Reynolds stresses":

$$\tau_{ij} = -\overline{\rho u_i' u_j'}. \tag{2.5}$$

Physically the "Reynolds stresses" represent the effects of turbulent mixing on the transport of heat, mass and momentum. Empirically-based turbulence models are then used to close the Reynolds-averaged equation set, either through simple algebraic expressions for Reynolds stresses or by the solution of additional transport equations. The most commonly-encountered RANS turbulence model is referred to as the $k-\varepsilon$ model [21]. k is turbulent kinetic energy, ε is the rate of dissipation of k, defined as:

$$k = \frac{1}{2}\left(\overline{u_i' u_i'} + \overline{u_j' u_j'} + \overline{u_k' u_k'}\right), \tag{2.6}$$

with u_i', u_j', u_k' the velocity fluctuating components, and

$$\varepsilon = k^{\frac{3}{2}} \ell^{-1}, \tag{2.7}$$

where ℓ is a turbulence characteristic length.

The model is based on the premise that the Reynolds stresses are linearly related to rates of local mean strain by means of a turbulent or "eddy" viscosity, which acts in an analogous manner to the physical viscosity of the fluid but depends on local flow conditions. Modifications to the basic $k-\varepsilon$ model have been introduced for fire applications to account for the buoyancy effects on turbulent mixing [22, 23]. They consist of adding a buoyancy-related term in the model equations so that the resulting computed Reynolds stresses behave more as expected in the presence of buoyant forces.

The values of k and ε are found by solving simplified model versions of their exact transport equations. The source terms for k and ε are given by:

$$S_k = G_k + G_B - \rho, \tag{2.8a}$$

$$S_\varepsilon = C_{1\varepsilon}\frac{\varepsilon}{k}(G_k + G_B) - C_{2\varepsilon}\rho\frac{\varepsilon^2}{k}, \tag{2.8b}$$

where G_k is the turbulence production due to shear and G_B is the production due to buoyancy.

The turbulent viscosity μ_t is given in terms of k and ε as:

$$\mu_t = C_\mu \rho \frac{k^2}{\varepsilon}, \tag{2.9}$$

with C_μ, $C_{1\varepsilon}$ and $C_{2\varepsilon}$ model constants.

2.1.2 Combustion modelling

The Eddy Break-Up model of Magnussen and Hjertager [24, 25] is based on the solution of species transport equations for reactant and product concentrations. The model assumes that: i) the combustion process can be represented as a single, one-step reaction; ii) the chemical reaction is infinitely fast compared to the mixing rate of the reactant species, and consequently the turbulence mixing of the gas phase reactants

controls the combustion rate. The model relates the rate of reaction to the dissipation rate of turbulent eddies containing products and reactants. The dissipation rate of turbulent eddies is assumed to be proportional to the ratio of the turbulent kinetic dissipation and the turbulent kinetic energy, ε/k [26]. The rate of reaction R_i is given by the smallest of the two expressions below [16]:

$$R_i = -\nu_i M_i A \rho \frac{\varepsilon}{k} \frac{m_R}{\nu_R M_R}, \tag{2.10a}$$

$$R_i = -\nu_i M_i A B \rho \frac{\varepsilon}{k} \frac{\sum_P m_P}{\sum_P \nu_P M_P}, \tag{2.10b}$$

where M_i denotes the molecular weight of species i, ν_R and M_R are the stoichiometric coefficients of the reaction, m_P are the mass fractions of any product species P, m_R represents the mass fraction of the reactant R, giving the smallest R_i, and A and B are empirical constants, i.e., $A = 4.0$ and $B = 0.5$.

The modelling of soot formation is based on a two-step process adapted by Magnussen [27] from the work of Tesner et al. [28]. The first step treats the formation of nuclei from gas phase and the second step treats the formation of soot particles from the nuclei. Once soot is formed, the model includes the combustion of the soot in the flame; the soot combustion rate is expressed from an Eddy Dissipation Concept model in terms of the dissipation rate and the turbulent kinetic energy k. The above model assumes that the rate of formation of soot depends on the mixing between the eddies that contain soot and other eddies that contain oxygen. The model, however, introduces only the particle number density and does not address the question of surface growth and of particle size evolution.

2.1.3 Radiation modelling

In the energy equation (2.3) the effect of radiation is accounted for by the use of a source term $-\nabla \cdot \mathbf{q_r}$, which must be supplied by a separate radiation model [7,19,29].

The fundamental quantity of radiation transport is the spectral radiation intensity I_ν, depending on position and direction. I_ν is defined as the radiant energy (per unit time and per unit wavelength interval) passing per unit surface area normal to the direction s into a unit solid angle Ω. The spectral radiative transfer equation (RTE) is a first order integro-differential equation for I_ν in a fixed direction, s,

$$\begin{aligned}\frac{dI_\nu(\mathbf{r},\mathbf{s})}{ds} =& -K_{a\nu} I_\nu(\mathbf{r},\mathbf{s}) - K_{s\nu} I_\nu(\mathbf{r},\mathbf{s}) + K_{a\nu} I_b(\nu,T) \\ &+ \frac{K_{s\nu}}{4\pi} \int_{4\pi} I_\nu(\mathbf{r},\mathbf{s}')\Phi(\mathbf{s}\cdot\mathbf{s}')d\Omega' + S,\end{aligned} \tag{2.11}$$

where v is the frequency, $\mathbf{s}$ and $\mathbf{r}$ are the direction and the position vectors, respectively, s is the path length, K_a and K_s are the absorption and the scattering coefficients, respectively, T is the local absolute temperature, I_b is the blackbody emission intensity that is proportional, according to the Stefan-Boltzmann law, to T^4, Φ is the in-scattering phase function giving the scattered intensity form direction $\mathbf{s}'$ to $\mathbf{s}$, and S is the relevant radiation intensity source term.

The spectral radiative heat flux, q_ν^R passing through a surface at some location $\mathbf{r}$ with a unit vector normal $\mathbf{n}$ is

$$q_\nu^R(\mathbf{r},\mathbf{n}) = \int (\mathbf{s}\cdot\mathbf{n}) I_\nu(\mathbf{r},\mathbf{s}) d\Omega_s. \tag{2.12}$$

Finally, the total radiative flux term in Eq. (2.3) is obtained by integrating Eq. (2.12) over solid angles and over the spectrum.

Descriptions of mathematical methods for solving the RTE are available in heat transfer textbooks [30–32]. Indeed, it is very difficult to solve in its general form, and a complete radiation model is very expensive. In problems where thermal radiation is significant, as for fires in enclosures, the proper choice of the radiation model will affect not only the quality of the solution, but also the computational time. In practice, there is a range of simplifying assumptions that may be appropriate for a given problem. A comprehensive comparison of six CFD methods for solving the RTE is reported by Jensen et al. [15] for the numerical simulation of a 2m diameter JP-8 pool fire. A detailed discussion on the models for radiation is also available in [3,16–18].

Among the different available modelling approaches, the most common used for large fires [3,29] are, in order of increasing complexity:

1. Fractional heat loss due to radiative heat transfer. This method is based on the observation that flames radiate a roughly fixed proportion of their total heat release, which depends on the type of the fuel and on fire scenario. Thus, this approach simply ignores in the simulation the percentage of the heat release rate (HRR) from a fire that turns into radiation, by reducing by 20-40% [3,9–11] the amount of HRR to be used in the energy balance equation, i.e., $\dot{Q}_R$ in Eq. (2.3);
2. Discrete Transfer model. This model, developed by Shah [33,34], is based on tracing the domain by multiple rays leaving from the bounding surfaces. The technique solves the radiative transfer equation along discrete representative "rays" of radiation traced in the computational domain for the radiation field, and its accuracy depends on the chosen ray directions as well as on the number of rays [7,16,19]. The physical quantities in each control volume crossed by a radiation ray are assumed to be uniform, and then the RTE equation can be integrated analytically. The Discrete Transfer model provides a good compromise between computational economy and precision; it is commonly and successfully applied to fire modelling problems, as reported for example by Novozhilov [7], Jensen et al. [15] and Wen et al. [35] who studied large compartment fires;
3. Monte Carlo model. The Monte Carlo method is a statistical method that simulates the underlying processes which govern the system of interest, i.e., the physical interactions between photons and their environment. It assumes the radiation field as a photon gas, and the intensity is proportional to the differential angular flux of photons "emitted" in (pseudo-) random directions. A large number of sample photons, typically thousands, need to be tracked through a computational domain for the radiation field to generate their histories, in order to get good estimates of the physical

quantities of interest [3, 19]. The photons are tracked in the Monte Carlo model in the same way that rays are traced through the domain in the Discrete Transfer model. By following a typical selection of photons and tallying, in each volume element, the relevant parameters, the mean total intensities and radiative flux can be calculated. The Monte Carlo method has been used for computation of radiation in compartment fires [36–38], although, given its computational cost, it is not generally applied to fires and smoke movement in large complex spaces. However, Snegirev et al. [31] claimed that it will be soon feasible, from a computational overhead point of view, to use the Monte Carlo method to this aim.

As concerns the radiative properties of combustion gases, absorption coefficient, scattering coefficient and refractive index may be a function of intensive thermodynamic variables such as temperature and pressure, as well as composition. Moreover, for non-grey media the radiation intensity field may be also a function of the spectrum as shown in Eq. (2.12) [19]. According to [7, 36, 39], for many engineering applications, reasonable results are obtained using simplified methods.

The validity of a grey gas assumption has been discussed in [40]. If the grey media assumption is made, predictions may significantly depend on how the effective emission/absorption coefficient is calculated. It can be either assumed constant or calculated to provide correct value for total emissivity of the mixture occupying a given control volume of the computational domain [36]. In the former case, the Grey model assumes that all radiation quantities are nearly uniform throughout the spectrum, consequently the radiation intensity is the same for all frequencies. This simplifies the radiation calculation considerably since only one radiative transfer equation must be solved [19]. However, a significant limitation of the Grey model in combustion calculations is that a single absorption coefficient is set, independent of the local gas composition. In the latter case, a more detailed treatment is offered by the Weighted Sum of Grey Gases (WSGG) model [7,8,13,19,36], which is the most widely used global model for the calculation of gas radiative properties in combustion systems [41]. WSGG model has been developed by Hottel and Sarofim [13] and improved by Modest [30]. Within this approach, the absorptivity of the mixture is approximated by the sum of component grey gas absorptivities weighted with a temperature dependent factor. This method is obviously more expensive computationally. More details on the mathematical approach can be found in [19,30,36].

In this work, two approaches (single effective absorption coefficient and Weighted Sum of Grey Gases, referred as Multigrey) were used and compared in modeling of full-scale tunnel fires.

2.1.4 Numerical methods

The governing equations of fluid flow cannot be solved analytically except in special, highly simplified cases. The task of CFD is to generate approximate solutions to these equations by a numerical approach. An iterative approach is required because of the non-linear nature of the equations [5, 19]. CFX code is based on the finite volume

method, i.e., the region of interest is divided into small sub-regions (control volumes). In the matter of space discretization, the advection schemes implemented in CFX can be expressed as [19]:

$$\phi_{ip} = \phi_{up} + \beta \nabla \phi \cdot \Delta \mathbf{r}, \tag{2.13}$$

where the subscript ip denotes evaluation at an integration point, ϕ_{up} is the value at the upwind node, and $\mathbf{r}$ is the vector from the upwind node to the ip. A value of $\beta = 0$ yields a first order Upwind differencing scheme, which is very robust [19, 42]. Such first order Upwind differencing scheme was used to run both small-scale and full-scale simulations. In the matter of time discretization a First Order Backward Euler scheme [19] was used. This discretization is robust, fully implicit, bounded, conservative first-order accurate in time, and does not have a time step size limitation.

With regard to the solution strategy, CFX uses a coupled solver [19], in which all the hydrodynamic equations are solved as a single system. The coupled solver is faster and more robust than the traditional segregated solver and fewer iterations are required to obtain a converged solution. The solution of each set of equations consists of two numerically intensive operations; for each time step: i) coefficient generation: the non-linear equations are linearized and assembled into the solution matrix; ii) equation solution: the linear equations are solved using an algebraic multigrid method, which is an iterative solver whereby the exact solution of the equations is approached during the course of several iterations. For the equation solution, CFX uses a particular implementation of algebraic multigrid called Additive Correction. The multigrid process involves carrying out early iterations on a fine mesh and later iterations on progressively coarser virtual ones. The results are then transferred back from the coarsest mesh to the original fine mesh. More details are reported in the literature [43].

2.2 The solid flame radiation model

The empirical "solid flame radiation model" aims to estimate the impact of radiation from pool fires to potential targets [20]. It assumes that: the pool is circular or nearly circular; the fire can be represented by a solid body of a simple geometrical shape and thermal radiation is emitted from its surface; non-visible gases do not emit much radiation. In summary [44], estimating the thermal radiation field surrounding a fire using the "solid flame radiation model" involves the following steps: 1) to characterize the geometry of the pool fire and its HRR; 2) to determine the radiative properties of the fire, the view factors and the effective emissive power of the flame; 3) to calculate the radiative heat flux to the target at a given location. This model has been widely applied for hazard calculations to assess radiation in case of fires occurring in industrial sites, both in open spaces [45] and between premises [46], and also in nuclear power plant [44].

The intensity of thermal radiation from a pool fire to a target for no-wind conditions is given by the following equation [20]:

$$\dot{q}'' = EF_{1\to 2}, \tag{2.14}$$

where E is the flame emissive power, $F_{1\to2}$ is the configuration view factor and $\dot{q}''$ is the incident radiative heat flux.

The effective emissive power E in terms of effective pool diameter D is given by an empirical correlation [20]:

$$E = 58 \times (10^{-0.00823D}). \tag{2.15}$$

The configuration view factor $F_{1\to2}$ is a purely geometric quantity, which is a function of target location and distance from fire L, flame height H_f, and fire diameter D. Flame height of the pool fire H_f is determined using the Heskestad correlation [47]:

$$H_f = 0.235\dot{Q}^{\frac{2}{5}} - 1.02D, \tag{2.16}$$

where $\dot{Q}$ is the heat release rate (HRR) of the fire.

The fire HRR can be determined by laboratory or field testing. In the absence of experimental data, the maximum HRR for the fire, is given by [48]:

$$\dot{Q} = \dot{m}''\Delta H_{c,eff} A_f (1 - e^{-k\beta D}), \tag{2.17}$$

where A_f is the horizontal burning area of the fuel, $\dot{m}''$ is the burning rate per unit area and per unit time, $\Delta H_{c,eff}$ is the effective heat of combustion and $k\beta$ is an empirical constant, given by the product of the extinction-absorption coefficient of the flame (k) and the mean-beam-length corrector (β), reported in the literature [48] in case of sufficient available data.

Calculations for assessing the impact of radiations from pool fire on potential targets were performed by using the solid flame model. Results are reported in the following Section 5 and compared with CFD predictions in order to evaluate the relative performances of the simple approximated solid flame radiation model and of numerical simulations.

3 Simulations

ANSYS CFX is a general-purpose flow solver code, which has been widely used and validated for many aspects of enclosure fire safety, smoke movement and combustion, e.g., in tunnels [49]. The CFX solver allows efficient parallel running for all the numerically intensive tasks, allowing to easily distribute the CFD calculation across multiple processors for any set of physics and mesh type [19]. The parallel run modes depends on the hardware and operating system.

In this work the MPI/MPICH2 procedure on Windows XP 32bit was used to distribute total runs into 4Pentium personal computers to execute parallel processing. The CPU clock frequency of each computer was 3GHz and the memory was 2GB. The overall parallel run procedure is divided into two steps: i) a partitioning step, where the MeTiS partitioning algorithm divided the mesh into four different partitions; ii) a running step, where the mesh partitions were solved by four (a master and three slave) processes working on its own partition.

3.1 Small scale fire

Preliminary simulations were run using the CFX code for a small-scale steady-state tunnel fire reported by Xue et al. [16]. The tunnel was 6m long, with rectangular cross section ($0.9 \times 0.3\text{m}^2$), made of insulating materials. The fire source was located 1.5m from the inlet section. The burner dimensions were $0.18 \times 0.15\text{m}^2$. Liquefied petroleum gas (LPG) was used as fuel, with a steady-state HRR of 3.15kW. Ambient temperature was 300K. Longitudinal ventilation of 0.13m/s was generated at the inlet tunnel section.

Firstly, a sensitivity study of the effect of mesh resolution on the solution stability and on the results accuracy was carried out. An in-depth discussion about the results of such a sensitivity analysis can be found in [50].

CFX simulations were run in the whole tunnel, using the following settings: i) an unstructured mesh, with 45,771 elements of various resolution; ii) 15,000 iterations as a maximum; 10^{-5} as residual convergence criterion; the upwind advection scheme; iii) the $k-\varepsilon$ turbulence model with wall function; the Eddy Dissipation model for combustion of a 70%propane-30%butane mixture; iv) the radiation was either not solved or modelled by Discrete Transfer or Monte Carlo model, in Grey assumption. The quality of simulation results was evaluated by comparison with available experimental data [16].

3.2 Full scale fire

Tunnel fires at full-scale were simulated under hypotheses, based on case studies reported in the literature, regarding road transportation of flammable liquids and possible accidents and fire events. Data concerning the distribution of hazardous materials flows for land transportation identify gasoline and LPG as those most frequently transferred by road [51]. Therefore, the major contribution to fire risk deriving from goods transportation on the roads is due to liquid fuels and LPG, which can cause flash fires, pool fires or even vapour cloud explosions [51]. Among various scenarios the one most likely to occur in the case of road transportation of liquid fuels (like gasoline) is a pool fire subsequent to a small, a medium or a catastrophic release (tanker collapse) [51].

Based on this background, a tunnel fire scenario was assumed. The tunnel investigated was a two-tube (each tube one-way) road tunnel along the Southern Italian A3 highway, between Pontecagnano and Salerno. It is the main highway for the transportation of goods in Southern Italy. The tunnel is about 800m long, with an arched cross section of 12m $\times$ 7m, and is not equipped with any emergency ventilation system, in compliance with the current Italian directives for tunnel safety (forced ventilation is mandatory in tunnels longer than 1km) [52]. Tunnel portals were assumed at atmospheric pressure and ambient temperature, 298K. A small release and a subsequent $2 \times 2\text{m}^2$ gasoline pool fire was supposed at the tunnel centre. According to data in the literature, the mass loss rate of a burning pool of gasoline is about

0.05kg/m^{2}s [48] and an "ultra ultra fast" growth rate can be assumed [53]. These data are consistent with experimental data collected in full scale fire tests performed in the Ofenegg tunnel, Switzerland, and reported in the literature [54]. Hence, in this work the HRR curve was imposed to rise rapidly (in 90s) up to 8MW, remaining constant for about 10min and, then, decaying exponentially within 30min. In this work, a 100m section of the tunnel, centred on the pool fire location, was modelled. The simulations were run in a quarter of the tunnel, due to longitudinal and transverse symmetry of the scenario, with the following numerical input data and assumptions: i) an unstructured mesh approach was used, with 76,143 cells and a finer grid resolution where strong local gradient of properties were expected; ii) the upwind advection scheme and the first order backward eulerian transient scheme were set; the integration time step was 0.1s when radiation was modelled and 1s otherwise, with maximum 10 iterative loops per time step; the residual convergence criterion was taken as 10^{-5}; parallel processing was executed; iii) the $k-\varepsilon$ model was used for turbulence, the Eddy Dissipation model was set for combustion reaction of the octane-air gaseous mixture; the Magnussen soot model was also set in a run and solved in conjunction with the combustion reaction; iv) the radiative heat transfer was either modelled by the Discrete Transfer model or the Monte Carlo model, in "surface to surface" or "participating media" mode, in Grey or Multigrey assumptions. The fractional radiative heat loss approach was also assessed by assuming a 30% reduction in HRR.

4 Results

4.1 Small scale fire

In Fig. 1 the results of simulations pertaining to laboratory-scale tunnel fire are reported and compared with experimental data. Temperature profiles along the height at the tunnel centreline are reported, at 0.6m upstream the fire (Fig. 1(a)) and at 1.8m and 3.6m downstream the fire (Figs. 1(b)) and 2(b), respectively). Due to the peculiar characteristics of the scenario (HRR of only 3.15kW, giving rise to a moderate increase of the temperatures except within the flame), radiative phenomena were of moderate relevance and, therefore, small differences were found between the predicted results when using different approaches. As an example, results reported in Fig. 1 show that modelling the heat transfer by radiation contributes to lowering predicted temperatures by about 5% with respect to values computed without any radiation model, especially in the upper hot gas layer, and also that predicted temperature profiles are similar regardless of the radiation model used (either Discrete Transfer or Monte Carlo).

Actually, calculated temperature profiles along the tunnel height do not rise as gradually as experimental data does, thus resulting in a different trend at intermediate levels and yielding a relatively poor prediction for the height of the interface between cold layer and smoke layer. This occurs both upwind the fire, where temperatures at intermediate tunnel levels are underestimated in comparison with experimental

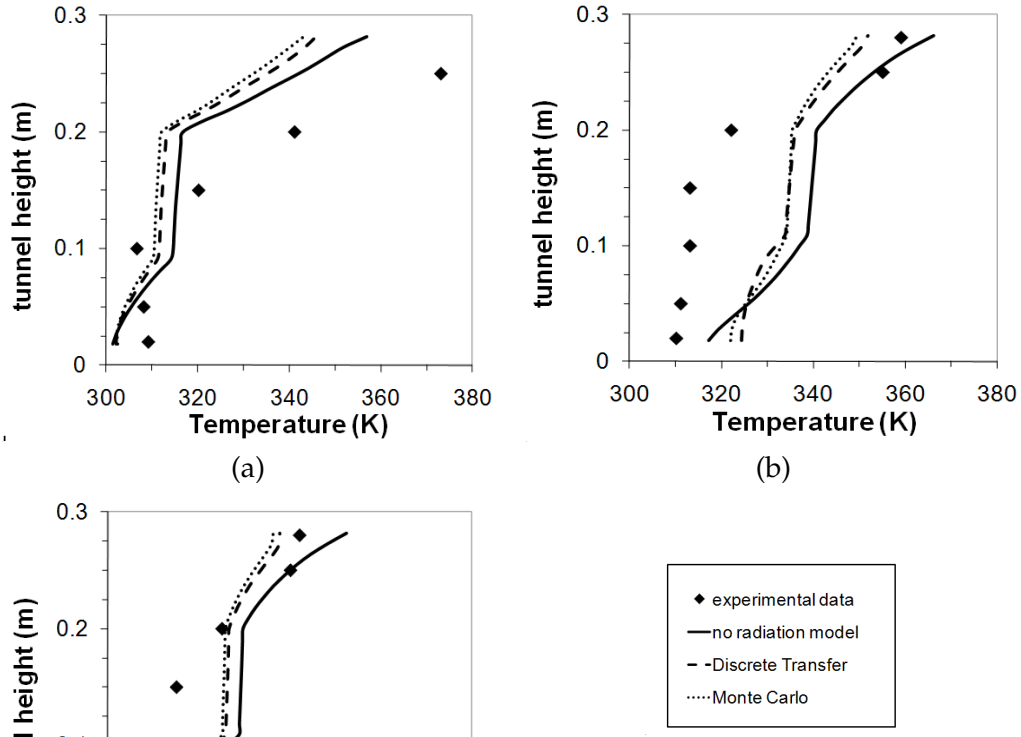

Figure 1: Small-scale tunnel fire. Temperature profiles along the height at the tunnel centerline: a) 0.6m upstream the fire; (b) 1.8m and (c) 3.6m downstream the fire.

data (Fig. 1(a)), and downstream the fire where, instead, they are overestimated. In particular, at the nearest downstream tunnel section (Fig. 1(b)) predicted temperatures are approximately 15-20K higher than experimental data along all the tunnel height up to about 0.2m, yielding an error of 5-6%. At the farthest section downstream the fire (see Fig. 1(c)), the simulated temperature is 325K at the height of about 0.1m, while experimental data shows that the temperature reaches such value at the height of 0.2m. Actually, a similar poor temperature prediction at intermediate heights downstream the fire was also reported by Hue at al. [16] who compared their own test data with those obtained by CFD simulations considering different combustion models.

On the whole, given the similar results regardless of the radiation model used, the Discrete Transfer model for radiation modelling was found to allow the best compromise between computing time and accuracy: it ensured a computational rate of 12.8 iterations/min and a good heat balance closure (90%) after 3200 iterations. Instead, with the Monte Carlo model the calculation rate was only 3.6 iterations/min and the program needed 8000 iterations for balances closure.

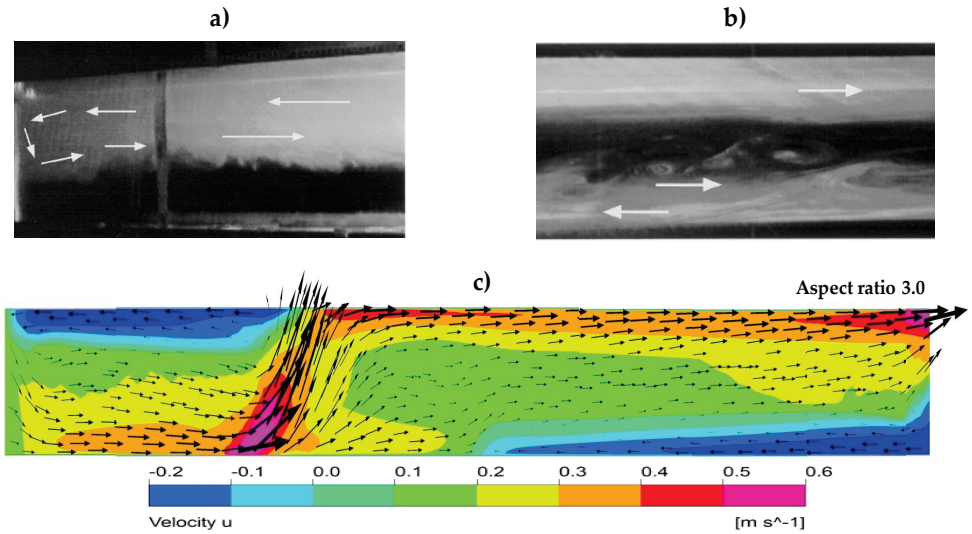

Figure 2: Small-scale tunnel fire. a) Experimental flow pattern upstream the fire. b) Experimental flow pattern downstream the fire. c) Predicted gas velocity distribution at the tunnel middleplane (Discrete Transfer run).

In Fig. 2(c) the gas flow velocity, calculated by Discrete transfer model at the tunnel middleplane, is reported. The model predicted a significant upstream back flow formed near the entrance section of the tunnel. Moreover, despite the longitudinal ventilation in the tunnel, a thin layer of recirculating flow near the floor that brings hot gases back against the ventilation is predicted. By comparing the simulation results (Fig. 2(c)) with experimental flow patterns upstream (Fig. 2(a)) and downstream (Fig. 2(b)) the fire, the main features of the experimental fire-induced airflow (upstream backflow (Fig. 2(a)), stratification (Figs. 2(a) and (b)) and recirculating flow downstream (Fig. 2(b))) are reproduced with reasonable agreement.

4.2 Full scale fire

In the case of the full-scale tunnel fire, simulations were performed in order to assess the effect of various models to take into account radiative heat transfer and of the radiation model parameters on the predicted gas temperatures. An outline of the simulations performed is reported in Table 1. The different models were evaluated in terms of reliability, consistency and computational run time.

Firstly, the Discrete Transfer (run II) and the Monte Carlo (run I) models were evaluated in the "participating media" Grey assumption with the gas absorption coefficients $a = 1\text{m}^{-1}$. As for the small-scale case, predicted temperature profiles are comparable each other regardless of the radiation model used. Indeed, differences between temperatures predicted by the two models (run I and II) at the end of the HRR growth phase (90s) were about 5K above and close to the pool, and almost negligible (less than 1K) far from the fire, with larger values computed by the Discrete Transfer

Table 1: Full-scale tunnel fire. Computational times for the growth phase (90s) with good balance closure, convergence and stability. (*) time step 1s instead of 0.1s.

Run	Radiation model/approach	Radiation transport mode	Radiative properties	Other	Computational time (fire growth phase)
I	Monte Carlo	Participating Media	$a = 1\text{m}^{-1}$		38.7h
II	Discrete Transfer	Participating Media	$a = 1\text{m}^{-1}$		9.5h
III	Discrete Transfer	Participating Media	$a = 0.08\text{m}^{-1}$		9.4h
IV	Discrete Transfer	Participating Media	$a = 0.2\text{m}^{-1}$		9.4h
V	Discrete Transfer	Participating Media	$a = 0.5\text{m}^{-1}$		9.4h
VI	Discrete Transfer	Participating Media	Multigrey		12.7h
VII	Discrete Transfer	Participating Media	Multigrey	Soot model	26h
VIII	Discrete Transfer	Surface to Surface			8h
IX (*)	No radiation model				1.5h
X (*)	30% HRR reduction				1.5h

model. However, the Monte Carlo model needed much more computational resource (about 4 times) compared to the Discrete Transfer model, as shown in Table 1, where the required computational times for the growth phase (90s) are reported for all the simulations run in this study.

Subsequently, using the Discrete Transfer participating media radiation model, a sensitivity analysis on the gas absorption coefficient in Grey (runs II-V) or Multigrey (run VI) assumption was performed. It results that while the flow pattern in the tunnel is similarly predicted regardless of the gas absorption coefficient used, this latter has significant effects on gas temperature. This is shown in Figs. 3(a) and (b), where the temperature profiles above the pool centre, predicted using various Grey or Multigrey assumptions, at the height of 1m and 3m, respectively, are reported.

The predicted gas layer temperature decreases as the gas absorption coefficient increases, with larger differences just above the pool (Fig. 3(a)). In particular, at the fire section it was found that when the fire is fully developed, predicted temperature within the flame decreases with a, the gas absorption coefficient, according to a third-order polynomial law. In the upper gas layer, predicted temperature varies slightly slower as a function of the absorption coefficient according to a power law with ex-

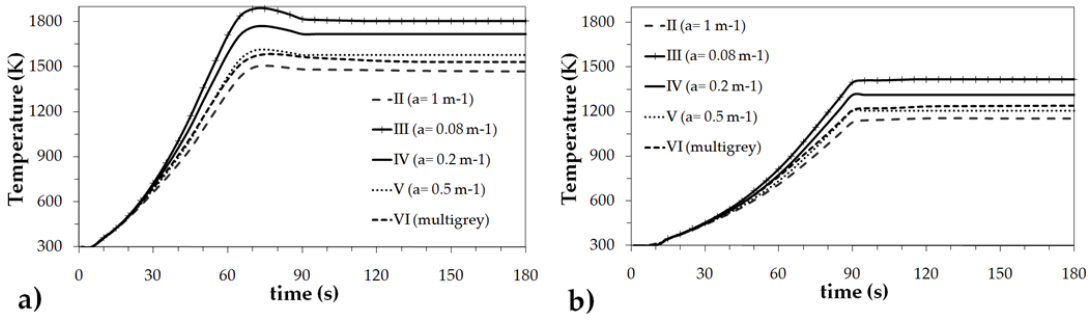

Figure 3: Full-scale tunnel fire. Time profiles of temperature above the pool centre: a) height 1m; b) height 3m.

ponent equal to -0.08. Conversely, far from the fire the differences between temperatures predicted using different absorption coefficient are negligible (below 5K). As shown in Figs. 3(a) and (b), when the gas absorption coefficient is assumed to be 0.5m^{-1} (run V), the simulated temperature profile mostly agrees with Multigrey behaviour (run VI). These results are in agreement with literature [55], where a constant (independent of the local gas composition) absorption coefficient over the whole domain has been employed with values in the range from 0.1 to 1m^{-1} in dependence on the characteristics of the fuel and of the scenario investigated.

The comparison between the required run times in Table 1 shows that the Grey model considerably simplifies the radiation transport calculation with respect to the more expensive Multigrey option, since fewer equations should be solved. However, for combustion calculations the use of the Grey model introduces errors in the total radiative heat flux [19]. Indeed, with this model the combustion air has the same radiative properties of the combustion products, although the latter can contain a high percentage of CO_2 and H_2O, which are highly efficient emitters of thermal radiation. This can lead to an overestimation of the absorption due to the air. Moreover, in enclosure fires both emission from gases and wall heating and reflection should be properly accounted for but, if the radiative heat transfer is modelled using the Grey spectral model, this effect is not correctly predicted [19]. On the other hand, a Multigrey model is able to give more reasonable gas absorption-emission characteristics resulting in fair agreement with measurements [55] and allowing the best compromise between computing time and result accuracy.

The effect of soot formation on the absorption coefficient and, therefore, on thermal radiation modelling was then assessed by solving the Magnussen soot model in conjunction with combustion, in the Discrete Transfer, Multigrey option (run VII). Generally, the formation of soot in gaseous flames can result both in significantly enhanced radiative heat transfer and in particulate pollution, mainly when in the reactant mixture the carbon to oxygen mole ratio is above unity [19]. In practice, due to the characteristics of the scenario (gasoline fuel, small pool size with respect to tunnel dimensions), soot production was of moderate extent, resulting in small differences in temperature (less than 10K) with respect to run VI and hence in radiation outputs. Moreover, as shown in Table 1, solving the soot model required a much longer computational time when compared to the corresponding case without soot (26h instead of 12.67h for the 90s growth phase).

Finally, the radiation transport "surface to surface" mode (run VIII) was also implemented in conjunction with the Discrete Transfer model and the results were compared with those relevant to run VI for Discrete Transfer with "participating media" Multigrey option. The results were also compared with those obtained with simulations carried out without radiation modelling (run IX) and with 30% reduction in the HRR (run X for the fractional heat loss approach).

Fig. 4 and Fig. 5 report the predicted temperature vertical profiles, on the tunnel centreline, 90s after the fire starting above the pool fire and at a distance of 25m downstream the fire, respectively.

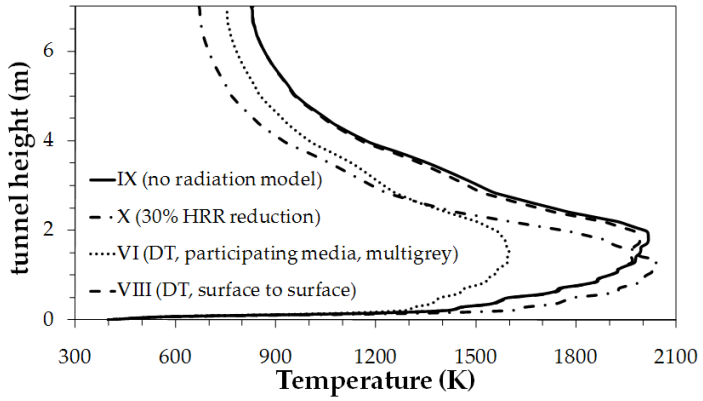

Figure 4: Full-scale tunnel fire. Temperature profiles above the pool, along the height and at the tunnel centreline, $t = 90$s.

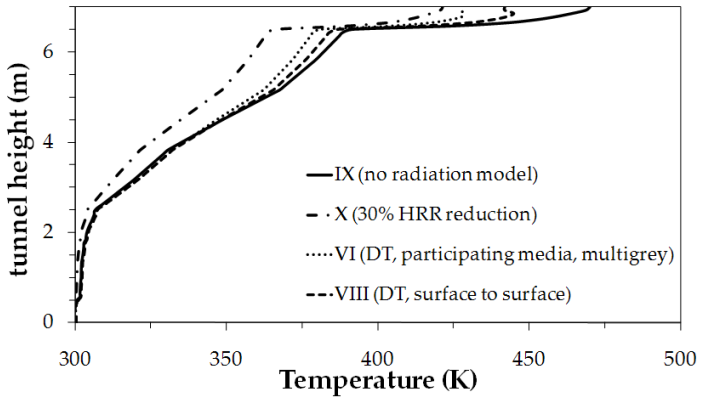

Figure 5: Full-scale tunnel fire. Temperature profiles at 25m from the fire, along the height and at the tunnel centreline, $t = 90$s.

Above the pool (Fig. 4) temperature values from all the simulations are consistent with the range of adiabatic flame temperature of gasoline-air mixtures (1632-2251K). At a distance of 25m from the fire (Fig. 5), the smoke and hot gases stratification is more stable being the predicted temperatures higher the upper the layer.

Results in Fig. 4 show that the temperatures above the fire predicted using the fractional radiative heat loss approach (run X) are, nearby the fire, comparable to those calculated without the use of any radiation model (run IX); but significantly lower as the vertical distance increases. In detail, at tunnel height less than 2m combustion occurs at flame temperature, and gas temperatures predicted in both runs IX and X reach approximately the same peak temperature of about 2030K, but at two different height above the pool 1.9m and 1.4m, respectively. Conversely, in the upper layer (>2m) great differences (about 200K) in the temperatures predicted in runs IX and X were observed.

On the contrary, the Discrete Transfer "surface to surface" radiation modelling (run VIII) yields temperature profiles above the pool (Fig. 4) practically coincident with

those obtained in the absence of radiation (run IX).

Finally, when radiation is modelled by Discrete Transfer Multigrey model (run VI) the gas temperatures within the flame and near the fire (i.e., up to 10m along the tunnel axis) are significantly lower than those calculated by imposing a reduced HRR (run X). As shown in Fig. 4, the Discrete Transfer Multigrey model (run VI) yields about a 20% reduction in maximum temperature, with a peak value of 1599K instead of 2030K. However, under the tunnel ceiling gas temperatures predicted by the Discrete Transfer Multigrey model (run VI) are approximately 85K higher than those calculated by the fractional heat release approach (run X), but are always lower (70-80K) than those computed in the cases of no radiation (run IX) and of Discrete Transfer "surface to surface" radiation modelling (run VIII). This because with the Multigrey option there is a lowering of the gas temperature as effect of the radiative heat emitted by hot gases generated by the combustion. The resulting reduction in temperature is in the range from 9% close to the ceiling to 22% close to the fire. These results could be interpreted also considering that the amount of hot gas production is directly proportional to the HRR and that, above and near the fire, domain gases are warmed up predominantly by the convective heat of combustion coming from the pool. Therefore, simulations give similar results when the HRRs are equal and there is not radiation heat emitted by the gas phase.

Results in Fig. 5 suggest that far from the fire there is not a dominant heat transfer mechanism, and convection and radiation become comparable; in fact, predicted temperatures in the case of radiation modelling (runs VI, VIII) are higher (about 10-20K) than those calculated by imposing a reduced HRR (run X) because of radiative heating of the ceiling and of gases, especially at elevated heights where hot gases are stratified (Fig. 5). In addition, the gas temperature profile along the tunnel height at 25m from the fire, obtained with the Discrete Transfer "surface to surface" radiative transfer model (run VIII), results in between those pertaining to the cases IX and VI of no radiation and of Discrete Transfer Multigrey, respectively (Fig. 5). Indeed, also at 25m from the fire, with equal HRR, the Discrete Transfer Multigrey model gives rise to the lowest vertical temperature profile and this behaviour, once again, is attributable to the cooling effect of the radiative heat emitted by the hot gases.

The ensemble of the results presented enables us to draw some considerations about the validity of the different ways employed in the present work to model thermal radiation in tunnel fires. The main consideration is that the results highlight the noticeable influence of radiation when considering large fires and the negligible effect of a such phenomenon if laboratory-scale fires are analyzed, as shown by temperature differences between those predicted by simulations without and with radiation model. Indeed, in case of full-scale tunnel fire such difference was on the order of 20-30%, whereas in case of small-scale was limited to 5-10%. This outcome is due to the larger heat release rates involved. In fact, the higher wall and gas temperatures resulting from the fire give rise to a significant radiation term according to the Stefan Boltzmann law (i.e., the total heat energy radiated from a body is proportional to the fourth power of its absolute temperature).

The simplest fractional radiative heat loss approach requires in less computational time (1/8) with respect to the other radiation models yielding a good (differences less than 10%) estimation of gas temperatures in the upper layer and at some distance from the fire. Indeed, these are the zone where the actual convective heat transport is the governing transfer mode. On the contrary, it overestimates (up to 30%) the gas temperatures close to the fire.

Generally, whenever a domain fluid does not emit/absorb radiation, the "surface to surface" transfer mode option should be chosen, since it reduces the computational time, as shown in Table 1. In any case, this transfer mode assumes that the domain fluid is like a transparent media, i.e., that radiative exchange only occurs between solid surfaces. Therefore the net radiation intensity will depend only on the total view factor between surfaces, on the total interchange area, and on surface properties and temperatures. As shown by simulation results, in modelling confined fires in tunnels this model may reproduce temperature profile likewise without any radiation model (see Fig. 4). This because the influence on radiation of the combustion products is not negligible, especially above the pool where the radiative heat transfer is mainly due to the fluid medium, rich of combustion gases. Hence, its use is not advisable. Moreover, owing to the assumptions on which the "surface to surface" model is based, the pertaining simulations give a single result over the whole domain in terms of incident radiation. This does not allow a correct evaluation of the pointwise radiant heat flux from a fire and the assessment of safety conditions within the tunnel (as reported in the following Section) and, therefore, represents a limit in the suitability of the use of CFD for Fire Hazard Analysis.

Finally, in modelling radiation and the effect of "participating media" like combustion gases the Gray approach, with the use of a constant absorption coefficient over the whole domain, may give significant differences in the results in dependence of the value of the absorption coefficient. Significant reduction (up to 20% for $a = 0.08\text{m}^{-1}$) of predicted temperatures in the fire zone with respect to Multigrey model are observed varying the gas absorption coefficient (Fig. 3). Moreover, with respect to Monte Carlo method, the Discrete Transfer Multigrey model requires lower computing time.

5 CFD in quantitative fire hazard analysis

In Fig. 6 results of CFD simulations in terms of radiant heat flux to a target at different heights and distances from the pool fire were compared with those obtained from empirical correlations, usually applied for fire risk assessment in buildings and public facilities ("solid flame radiation model" [20, 44]).

It appears that, except at small distances from the fire ($<$3m), the incident radiation values computed by simulations overestimate those yielded by the empirical correlations and, hence, they are more conservative with a view to FHAs. Moreover, correlations are based on assumptions (e.g., pool size, flame height and shape, time-averaged size of the visible envelope, average emissive power, wind, enclosure size) that limit

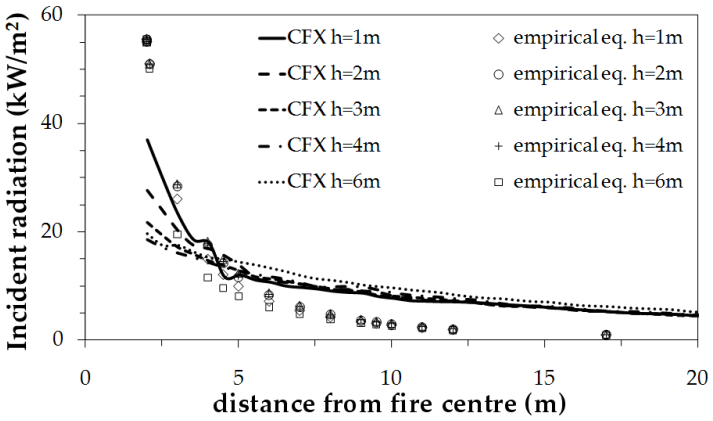

Figure 6: Full-scale tunnel fire. Incident radiation flux calculated by CFD simulations and by empirical correlations at different distances and heights (h) from the pool fire, $t = 90$s.

their applicability, and have inherent limitations in their predictive capabilities. On the contrary, CFD models, when validated through suitable tests, are applicable to a wider range of conditions and scenarios [3,6,10,16,19,55].

In the context of Fire Hazard Analysis, the hypothesized full-scale tunnel fire scenario was also studied from the point of view of tenability conditions within the tunnel in the time.

Generally, during a tunnel fire people's lives are threatened in a number of ways by the hot smoke spreading. The accepted target criteria for tunnel users and fire-fighters are [56]: (i) to provide survivable gas temperatures, i.e., not exceeding 60°C (100°C for fire-fighters); (ii) to contain radiation heat flux below 2kW/m^2 (5KW/m^2 for fire-fighters); (iii) to keep pollutants and toxic species concentrations below dangerous values, that is below the Immediately Dangerous to Life or Health (IDLH) concentrations: IDLH is 40,000ppm for CO_2 and 1,200ppm for CO; (iv) to guarantee a minimum O_2 concentration (16vol %) to allow breathing without impairing thinking and coordination; to control smoke and, hence, visibility: illuminated signs should be discernible at 10m.

In fact, as concerns the hypothesized tunnel fire scenario with a small gasoline release and a relatively moderate fire, the hazard mainly derives from people exposure to hot temperature and large radiative heat flux. Indeed, stratification is stable and smoke remains confined in the upper layer below the tunnel ceiling, and CO_2 and CO concentrations and O_2 consumption are almost negligible at breathing level along the tunnel length (except above the pool). The time profiles of gas temperature and incident radiation, predicted by the simulation at the average breathing height of 2m and on the tunnel centreline are shown in Fig. 7 and Fig. 8, respectively. Results are reported for people located at various distances from the fire (2.5, 5, 10, 15, 20m), and compared with the accepted safety values for tunnel users and for fire-fighters.

With regard to gas temperature (Fig. 7), hazardous values for unprotected people are reached at eye level about 3min after the fire starting at distances up to 10m from

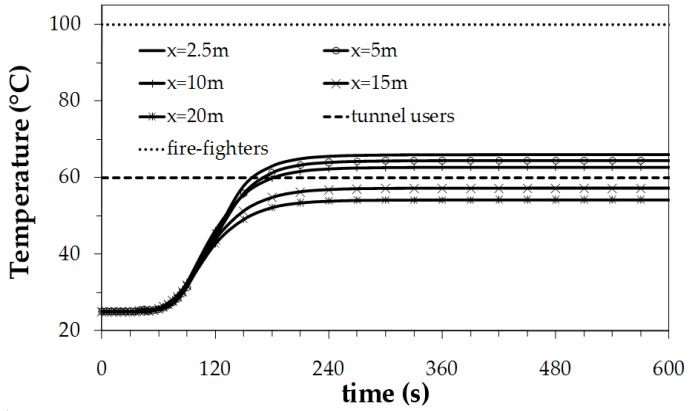

Figure 7: Full-scale tunnel fire. Temperature profiles along the time at the height of 2m and at the tunnel centreline, at different distances from the pool fire, in comparison with safety values.

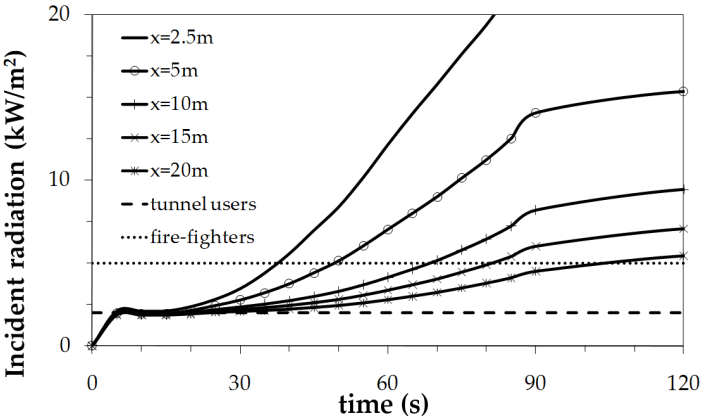

Figure 8: Full-scale tunnel fire. Incident radiation profiles along the time at the height of 2m and at the tunnel centreline, at different distances from the pool fire, in comparison with safety values.

the pool. However, temperatures level off towards a value which is only a little higher than 60°C. Conversely, the temperature remains always below the safety limit along the tunnel section far from the fire (i.e., for $x \geq 15$m, Fig. 7). Therefore such results show that for the hypothesized scenario temperature exposure represents a relatively small hazard for people.

On the other hand, results in terms of incident radiation highlight the severe risk, deriving from the radiative heat emitted by the pool fire, for both tunnel users and fire-fighters exposed along the tunnel up to 20m far from the fire. The radiation intensity stays on the border of safety limits in the initial fire phase but, afterwards, the radiative flux reaches hazardous values, able to cause severe burns and injuries if people do not start to escape towards tunnel portals. Even protected fire-fighters will be able to contrast the fire only from distances larger than 20m. Hence, radiation demonstrates to be a significant hazard for people, even for the hypothesized scenario with a relatively small fire.

6 Conclusions

In this work CFD modelling was adopted to simulate small-scale and full-scale pool fires in tunnels and to assess for this case the relative influence of heat transfer by convection and by radiation.

Radiation proved to be a significant phenomenon above all in the case of large scale fires, so it should be properly taken into account to achieve reliable predictions by numerical simulations.

Results of our simulations showed that the use of fractional radiative heat loss approach is advisable only to have an approximate and rapid estimation of probable temperature profiles in the tunnel in the upper layer and at some distance from the fire; whereas, in the proximity of the fire it gave results similar to those obtained without modelling radiation. The worst results were obtained by the surface to surface radiation model.

Among the tested radiation models, Monte Carlo and Discrete Transfer model gave similar temperature predictions, but the latter required lower computing time. Moreover, the effect of participating media like combustion gases and the dependence of the gas radiation properties on temperature (multigrey model) may not be neglected. Indeed, the use of a constant absorption coefficient over the whole domain (Gray approach) may give significant differences in the results in dependence of the value of the absorption coefficient. For the scenario investigated a value of the absorption coefficient equal to 0.5 gave results close to those obtained by the multigrey model.

Finally, the suitability of the use of CFD in quantitative FHA of full-scale tunnel fire scenarios have also been highlighted. Radiant heat flux proves to be a noteworthy hazard for exposed people, even when the fire is of moderate extent, such as in the hypothesized scenario of a small gasoline release generating a pool fire with a maximum HRR of 8MW.

Nomenclature

Constants

g	gravitation acceleration	$9.81\mathrm{m/s^2}$
σ	Stefan Boltzmann constant	$5.67 \times 10^{-8}\mathrm{W/m^2K^4}$

Variables

a	absorption coefficient	$\mathrm{m^{-1}}$
A	area	$\mathrm{m^2}$
D	diameter	m
D_j	diffusion coefficient of j-th species into air	$\mathrm{m^2/s}$
E	flame emissive power	$\mathrm{W/m^2}$
$F_{1\to 2}$	configuration view factor	

h	specific enthalpy	J/kg
H	height	m
$\Delta H_{c,eff}$	effective heat of combustion	J/kg
I_b	blackbody emission intensity	W/m^2
I_ν	spectral radiation intensity	$W \cdot sr^{-1}$
k	thermal conductivity	W/mK
k	turbulent kinetic energy	J
k	extinction-absorption coefficient of the flame	m^{-1}
K_a	absorption coefficient	m^{-1}
K_s	scattering coefficient	m^{-1}
ℓ	turbulence characteristic length	m
L	distance	m
M	molecular weight	g/mol
$\dot{m}''$	burning rate per unit area per unit time	kg/m^2s
P, p	pressure	Pa
q	heat flux	W/m^2
q_ν^R	spectral radiative heat flux	W/m^2
$\dot{Q}$	heat release rate (HRR)	W
$\dot{Q}_R$	heat release rate per unit volume	W/m^3
$\mathbf{r}$	position vector	m
R	rate of reaction	mol/s
$\mathbf{s}$	direction vector	m
s	path length	m
T	temperature	K or °C
t	time	s
$\mathbf{u}$, $u_i(v_i)$	velocity, velocity components	m/s
x, x_i	cartesian positions	m
Y	mixture fraction	-

Greek Symbols

β	mean-beam-length corrector	
β'	coefficient for advection schemes	
ε	rate of dissipation of turbulent energy k	m^2/s^3
ϕ	generic scalar fluid variable	
ϕ'	fluctuating part of a variable	
$\overline{\phi}$	non-fluctuating part of a variable	
μ	gas dynamic viscosity	Pa s
μ_t	turbulent viscosity	kg/ms
v	frequency	s^{-1}
ν	molar stoichiometric coefficients of the reaction	
Ω	unit solid angle	rad
Φ	in-scattering phase function	
ρ	density	kg/m^3

τ	shear stress	N/m^2

Subscripts

0	free stream/ambient/initial
f	flame
i, j	chemical species
i, j, k	component
ip	integration point
P	product
r	radiative
R	reactant
t	turbulent
up	upwind node

References

[1] F. VUILLEUMIER, A. WEATHERILL AND B. CRAUSAZ, *Safety aspect of railway and road tunnel: example of the Lötschberg railway tunnel and Mont-Blanc road tunnel*, Tunn. Undergr. Sp. Tech., 17 (2002), pp. 153–158.

[2] M. J. HURLEY AND R. W. BUKOWSKI, Fire Hazard Analysis Techniques, Fire Protection Handbook, 20th Edition (A. E. Cote et al. Eds.), National Fire Protection Association, Quincy (USA), 2008.

[3] N. GOBEAU, H. S. LEDIN AND C. J. LEA, *Guidance for HSE inspectors: smoke movement in complex enclosed spaces-assessment of computational fluid dynamics*, HSL Report 29, 2002.

[4] C. T. SHAW, Using Computational Fluid Dynamics, Prentice Hall, London (UK), 1992.

[5] C. J. LEA, *Guidance for NSD on the assessment of CFD simulations in safety cases*, HSL Report FS/97/8, 1997.

[6] A. KASHEF, N. BÉNICHOU AND G. LOUGHEED, *Numerical modelling and behaviour of smoke produced from fires in the Ville-Marie and L.-H.-La Fontaine Tunnels: literature review*, NRCC Report IRC-RR-141, 2003.

[7] V. NOVOZIHILOV, *Computational fluid dynamics modelling of compartment fires*, Prog. Energ. Combust., 27 (2001), pp. 611–666.

[8] J. F. SACADURA, *Radiative heat transfer in fire safety science*, J. Quant. Spectrosc. Ra., 93 (2005), pp. 5–24.

[9] A. TEWARSON, Generation of Heat and Chemical Compounds in Fires, SFPE Handbook of Fire Protection Engineering, 2nd Edition (P. J. DiNenno et al. Eds.), National Fire Protection Association, Quincy (USA), 1995.

[10] P. J. WOODBURN AND R. E. BRITTER, *CFD simulation of a tunnel fire-part I*, Fire. Safety. J., 26 (1996), pp. 35–62.

[11] O. MÉGRET AND O. VAUQUELIN, *A model to evaluate tunnel fire characteristics*, Fire. Safety. J., 34 (2000), pp. 393–401.

[12] C. L. TIEN, K. Y. LEE AND A. J. STRETTON, Radiation Heat Transfer, SFPE Handbook of Fire Protection Engineering, 2nd Edition (P. J. DiNenno et al. Eds.), National Fire Protection Association, Quincy (USA), 1995.

[13] H. C. HOTTEL AND A. F. SAROFIM, Heat Transfer by Radiation, Perry's Chemical Engineers' Handbook, 7th Edition (R. H. Perry et al. Eds.), McGraw-Hill, New York (USA), 1997.
[14] E. P. KERAMIDA, A. G. BOUDOUVIS, E. LOIS, N. C. MARKATOS AND A. N. KARAYANNIS, *Evaluation of two radiation models in CFD fire modeling*, Numer. Heat. Trans. A. Appl., 39 (2001), pp. 711–722.
[15] K. A. JENSEN, J. F. RIPOLL, A. A. WRAY, D. JOSEPH AND M. EL HAFI, *On various modeling approaches to radiative heat transfer in pool fires*, Combust. Flame., 148 (2007), pp. 263–279.
[16] H. XUE, J. C. HO AND Y. M. CHENG, *Comparison of different combustion models in enclosure fire simulation*, Fire. Safety. J., 36 (2001), pp. 37–54.
[17] R. A. HART, Numerical Modelling of Tunnel Fires and Water Mist Suppression, PhD thesis, University of Nottingham (UK), 2005.
[18] J. WANG, J. HUA, K. KUMAR AND S. KUMAR, *Evaluation of CFD modelling, methods for fire induced airflow in a room*, J. Fire. Sci., 24 (2006), pp. 393–411.
[19] ANSYS, CFX help, Release 12.0, 2009.
[20] C. L. BEYLER, Fire Hazard Calculations for Large Open Hydrogen Fires, SFPE Handbook of Fire Protection Engineering, 3rd Edition (P. J. DiNenno et al. Eds.), National Fire Protection Association, Quincy (USA), 2002.
[21] B. E. LAUNDER AND D. SPALDING, *The numerical computation of turbulent flows*, Comput. Method. Appl., 3 (1974), pp. 269–289.
[22] W. RODI, *Influence of buoyancy and rotation on equations for the turbulent length scale*, Proc. of the 2nd Symp. on Turbulent Shear Flows, London (UK), July 2-4, 1979.
[23] N. C. MARKATOS, M. R. MALIN AND G. COX, *Mathematical modeling of buoyancy-induced smoke flow in enclosures*, Int. J. Heat. Mass. Trans., 25 (1982), pp. 63–75.
[24] B. F. MAGNUSSEN AND B. H. HJERTAGER, *On mathematical models of turbulent combustion with special emphasis on soot formation and combustion*, Proc. of the 16th Int. Symp. on Combustion, Cambridge (USA), August 15-20, 1976.
[25] B. F. MAGNUSSEN, B. H. HJERTAGER, J. G. OLSEN, AND D. BHADURI, *The eddy dissipation concept*, Proc. of the 17th Int. Symp. on Combustion, Leeds (UK), August 20-25, 1978, pp. 1383–1398.
[26] D. B. SPALDING, *Mixing and chemical reaction in steady confined turbulent flames*, Proc. of the 13th Int. Symp. on Combustion, Salt Lake City (USA), August 23-29, 1970, pp. 649–657.
[27] B. F. MAGNUSSEN, Particulate Carbon Formation During Combustion, Plenum Publishing Corporation, 1981.
[28] P. A. TESNER, T. D. SNEGIRIOVA, AND V. G. KNORRE, *Kinetics of dispersed carbon formation*, Combust. Flame., 17 (1971), pp. 253–271.
[29] R. VISKANTA, *Overview of some radiative transfer issues in simulation of unwanted fires*, Int. J. Therm. Sci., 47 (2008), pp. 1563–1570.
[30] M. F. MODEST, Radiative Heat Transfer, 2nd Edition, Academic Press, Amsterdam, 2003.
[31] R. SIEGEL AND J. R. HOWELL, Thermal Radiation Heat Transfer, 4th Edition, Francis & Taylor, New York, 2002.
[32] G. C. POMRANING, The Equations of Radiation Thermodynamics, Pergamon, 1992.
[33] N. G. SHAH, The Computation of Radiative Heat Transfer, PhD Thesis, University of London (UK), Faculty of Engineering, 1979.
[34] F. C. LOCKWOOD, AND N. G. SHAH, *A new radiation solution method for incorporation in general combustion prediction procedures*, Proc. of the 18th Int. Symp. on Combustion, Pittsburgh (USA), August 17-22, 1980, pp. 1405–1414.

[35] J. X. WEN, L. Y. HUANG AND J. ROBERTS, *The effect of microscopic and global radiative heat exchange on the field predictions of compartment fires*, Fire. Safety. J., 36 (2001), pp. 205–223.
[36] A. YU. SNEGIREV, *Statistical modeling of thermal radiation transfer in buoyant turbulent diffusion flames*, Combust. Flame., 136 (2004), pp. 51–71.
[37] A. YU. SNEGIREV, G. M. MAKHVILADZE, AND V. A. TALALOV, *Statistical modelling of thermal radiation in compartment fire*, 9th Int. Fire Science & Engineering Conf. (Interflam 2001), Edinburgh (Scotland), September 17-19, 2001, pp. 1011–1024.
[38] J. ZHANG, O. GICQUEL, D. VEYNANTE AND J. TAINE, *Monte Carlo method of radiative transfer applied to a turbulent flame modeling with LES*, C. R. Mecanique., 337 (2009), pp. 539–549.
[39] D. F. FLETCHER, J. H. KENT, V. B. APTE AND A. R. GREEN, *Numerical simulations of smoke movement from a pool fire in a ventilated tunnel*, Fire. Safety. J., 23 (1994), pp. 305–325.
[40] J. DE RIS, *Fire radiation-a review*, Proc. of the 17th Int. Symp. on Combustion, Leeds (UK), August 20-25, 1978, pp. 1003–1016.
[41] P. J. COELHO, *Numerical simulation of the interaction between turbulence and radiation in reactive flows*, Prog. Energ. Combust., 33 (2007), pp. 311–383.
[42] T. J. BARTH AND D. C. JESPERSON, *The design and application of upwind schemes on unstructured meshes*, Proc. of the 27th Aerospace and Sciences Meeting, Reno (USA), January 9-12, 1989, AIAA Paper 89-0366.
[43] M. J. RAW, *Robustness of coupled algebraic multigrid for the Navier-Stokes equations*, Proc. of the 34th Aerospace and Sciences Meeting & Exhibit, Reno (USA), January 15-18, 1996, AIAA paper 96-0297.
[44] N. IQBAL, M. H. SALLEY AND S. WEERAKKODY, Fire Dynamics Tools (FDTs)-Quantitative Fire Hazard Analysis Methods for the U.S. Nuclear Regulatory Commission Fire Protection Inspection Program (NUREG-1805), 2004.
[45] K. MCGRATTAN, H. R. BAUM AND A. HAMINS, Thermal Radiation from Large Pool Fires, Report NISTIR 6546, 2000.
[46] A. LÖNNERMARK AND H. INGASON, *Fire spread between industry premises*, SP Report 2010: 18, 2010.
[47] G. HESKESTAD, Fire Plumes, SFPE Handbook of Fire Protection Engineering, 2nd Edition (P. J. DiNenno et al. Eds.), National Fire Protection Association, Quincy (USA), 1995.
[48] V. BABRAUSKAS, Burning Rates, SFPE Handbook of Fire Protection Engineering, 2nd Edition (P. J. DiNenno et al. Eds.), National Fire Protection Association, Quincy (USA), 1995.
[49] S. JAIN, S. KUMAR, S. KUMAR AND T. P. SHARMA, *Numerical simulation of fire in a tunnel: comparative study of CFAST and CFX predictions*, Tunn. Undergr. Sp. Tech., 23 (2008), pp. 160–170.
[50] M. G. MEO, Modelling of Enclosure Fires, PhD thesis in Chemical Engineering, University of Salerno (Italy), 2009, available online at `http://www3.unisa.it/uploads/1270/38._tesi_maria_grazia_meo.pdf`.
[51] M. F. MILAZZO, R. LISI, G. MASCHIO, G. ANTONIONI, S. BONVICINI AND G. SPADONI, *HazMat transport through Messina town: from risk analysis suggestions for improving territorial safety*, J. Loss. Prevent. Proc., 15 (2002), pp. 347–356.
[52] Decreto Legislativo 5 ottobre 2006, n. 264, Attuazione della direttiva 2004/54/CE in materia di sicurezza per le gallerie della rete stradale transeuropea.
[53] D. D. EVANS, Ceiling Jet Flows, SFPE Handbook of Fire Protection Engineering, 2nd Edition (P. J. DiNenno et al. Eds.), National Fire Protection Association, Quincy (USA), 1995.

[54] A. HAERTER, *Fire tests in the Ofenegg-Tunnel in 1965*, Proc. of the Int. Conf. on Fires in Tunnels, Borås (Sweden), October 10-11, 1994, pp. 195–214.

[55] J. HUA, J. WANG, K. KUMAR AND S. KUMAR, *Evaluation of the combustion and thermal radiation modelling methods for fuel- and ventilation-controlled compartment fires*, Proc. of the 10th Int. Fire Science & Engineering Conf. (Interflam 2004), Edinburgh (Scotland), July 5-7, 2004, pp. 787–794.

[56] CFPA-E 2009, *Fire safety engineering concerning evacuation from buildings*, European Guideline No 19: 2009.